IEEE Access
Multidisciplinary | Rapid Review | Open Access Journal

Received June 18, 2019, accepted July 13, 2019, date of publication July 17, 2019, date of current version August 5, 2019.

Digital Object Identifier 10.1109/ACCESS.2019.2929585

High Sensitive Capacitive Sensing Method for Thickness Detection of the Water Film on an Insulation Surface

NAN LI[1], (Member, IEEE), MINGCHEN CAO[2], XIAOJUN YU[1], JIABIN JIA[3], (Member, IEEE), AND YUNJIE YANG[3], (Member, IEEE)

[1]School of Automation, Northwestern Polytechnical University, Xi'an 710071, China
[2]State Key Laboratory for Manufacturing Systems Engineering, Xi'an Jiaotong University, Xi'an 710049, China
[3]School of Engineering, The University of Edinburgh, Edinburgh EH9 3FB, U.K.

Corresponding author: Nan Li (nan.li@ homail.co.uk)

This work was supported in part by the National Natural Science Foundation of China under Grant 51875477 and Grant 51475013, in part by the Top International University Visiting Program for Outstanding Young Scholars of Northwestern Polytechnical University, and in part by the China Scholarship Council under Grant 201806295037.

ABSTRACT Water films are always formed on the outer or inner surfaces of materials in industrial processes and some key parts of instruments because of complex working environments (moisture and hidden water). This situation may lead to inaccurate measurement results or even unsafety process for instrument operation. Therefore, it is important to reliably detect and quantify the formed water films. A coplanar capacitive sensor and an AD7745-based measurement system were designed for the first stage of this paper. A glass tank and a specific power ultrasonic humidifier were then added to construct the experimental platform. To verify the feasibility of the designed coplanar capacitive sensor, the thickness of the water films was set to change from 0 to 1.5 mm with a 0.1-mm interval. The experimental results based on the self-developed system were compared with the results simulated by COMSOL, and the results derived from Agilent 4294A (an impedance analyzer). The results indicated that the coplanar capacitive sensor could be used to detect and evaluate the thickness of the water film. The resolution of AD7745-based measurement system for water film thickness detection is less than 0.1 mm.

INDEX TERMS Coplanar capacitive sensor, water film, thickness detection, system design, resolution.

I. INTRODUCTION

Water film in all forms (moisture, hidden water, water droplets, etc.) always exists in specific industrial processes and some key parts of instruments. These liquid films form on the outer/inner surfaces of the materials, which may lead to unexpected corrosion or inaccurate measurement results, especially for complex working environments. It is necessary to detect the existence of the water film and evaluate its quantity. There are many detection methods that can be applied for liquid detection in various applications [1]–[4].

As a non-destructive and non-intrusive technique, the capacitive sensing technique has been developed and applied for a long period. Noltingk applied this technique to perform high precision measurement as early as 1969 [5]. Fringe capacitance frequently exists in practical capacitive sensor design and it sometimes leads to unexpected effects on sensor performance. In another aspect, the fringe capacitance effect causes nonlinear electric field distribution, which in turn causes coplanar sensor to have higher sensitivity. Thus, the coplanar capacitive sensing technique has been applied to many detection fields [6], [7]. Sundara-Rajan designed an interdigital capacitive sensor to determine the moisture concentration in paper pulp, and the repeatability and reproducibility tests indicated that the measurement results were accurate and reliable [8]. Nassr et al. used coplanar capacitive sensing technique to evaluate the water intrusion in composite structures. They pointed out that the sensor geometry had the greatest effect on the sensor performance, and the sensitivity of the designed sensor could easily identify the changes for water intrusion depths between 2 mm and 10 mm [9]. Matiss presented a coplanar capacitive sensor based method to complete the dielectric permittivity and thickness of a dielectric-plate/shell measurement [10]. Moreover, recently research studies have indicated that the capacitive sensor has the potential to be used in biomedical projects [11], [12] and

The associate editor coordinating the review of this manuscript and approving it for publication was Jaime Lloret.

environmental monitoring [13], [14] due to its high sensitivity and low cost. Therefore, more and more research works aim to develop new coplanar capacitive sensor structures or a method for making a high precision capacitive sensor. An inkjet-printed coplanar capacitive sensor in microscale was produced by Yang et al. for water level and quality monitoring. The sensitivity of the sensor was 1.9 pF/mm, which was much higher than that in previously reported works [15]. Lim et al. developed a capacitive humidity sensor with coplanar electrode structures. The sensor used PTB7-T with a facile solution processing approach, and it had a greater change in capacitance at low frequencies when compared to high frequencies with better sensitivity, good linearity, and fast response and recovery times [16]. Chetpattananondh et al. developed an interdigital capacitive sensor to measure the water level. The sensor was proven to measure absolute levels of water with a 0.2 cm resolution over a 30-cm range, which was sensitive enough to trace the variability of the water level [17]. A novel electrode structure named the serpentine electrode (SRE) was designed for the application of humidity measurement by Rivadeneyra et al. The performance of the SRE sensor was compared with that of the sensor in the interdigitated electrode structure. The authors believed that the new structure could also be used in the field of signal transduction due to its larger geometrical capacitance factor [18]. Considering the nonlinearity of the electrical field distribution of the coplanar capacitive sensor, some researchers tried to find an effective mathematical equation to calculate the capacitance of the designed capacitive sensor, but these researchers were more interested in experimental studies. Li et al. studied the capacitive imaging application using a multi-electrode capacitive sensor. The designed sensor was used to detect defects in the insulation layer and the metal surface, and the penetration depth and the signal strength were discussed [19]. Sheldon et al. applied the capacitive sensing technique to measure the permittivity of wire insulation materials, and they presented a new equation to calculate the capacitance. The mean difference between the calculated capacitance and that measured experimentally was found to be $< 2\%$ [20]. Yin et al. presented an equation to calculate the measurement sensitivity distribution of a coplanar capacitive imaging probe that consisted of two back-to-back triangular electrodes [21]. Our previous works also indicated that the coplanar capacitive sensing technique was a potential method for the quality evaluation of post-tensioned pre-stressed ducts [22].

In this paper, the coplanar capacitive sensing technique is studied for application to the thickness detection of a water film on an insulation surface. The structure and the working principle of a coplanar capacitive sensor are introduced, and the sensor performance including the sensor penetration depth and signal strength are defined first. An AD7745 based system was designed for measuring purposes. This system is introduced in Section 2. An experimental platform was established that consisted of a glass tank and a specific power ultrasonic humidifier. In Section 3, the thickness of the studied water film changes from 0 mm to 1.5 mm. Later in Section 3, the self-developed system is compared with the results simulated by COMSOL and the results derived from Agilent 4294A (the impedance analyzer). The conclusions are given in Section 4.

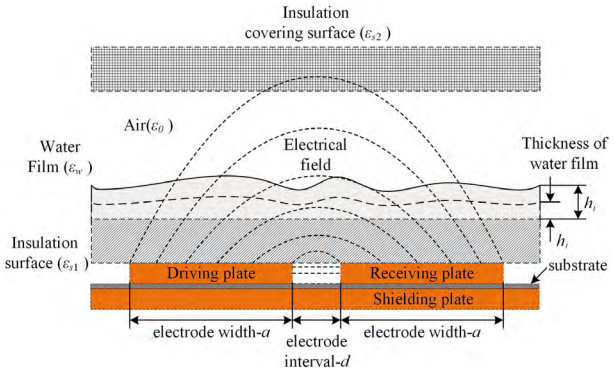

FIGURE 1. Sensing principle of a dual-plate coplanar capacitive sensor for the thickness detection of the water film on an insulation surface.

II. PRINCIPLES AND METHODOLOGY

A. SENSING AND CAPACITANCE MEASUREMENT PRINCIPLES

A dual-plate coplanar capacitive sensor consists of two metal electrodes, a driving plate and a receiving plate. The two electrodes are placed under the insulation surface. An AC excitation is supplied to the sensor and a nonlinear electrical field is then formed between the driving the receiving electrodes. A shielding plate is arranged under the sensing electrodes to suppress noise. Measurement values are determined by changes of the permittivity of the sensing materials above the sensor. The working principle of the sensor is shown in Fig. 1. The objects in the sensing area consist of insulation surface, water film, air, and an insulation covering surface. The permittivities of the insulation surface (ε_{s1}), water film (ε_w), air (ε_0), and insulation covering surface (ε_{s2}) can be seen as a new material with a mixed permittivity (ε_r). Because the thicknesses of the insulation surface and the covering surface are fixed, it is easy to conclude that the change in water film thickness is the only source of measurement change.

The capacitance measurement circuit is another key part of the entire inspection system. It affects the effectiveness and reliability of the whole detection system. At present, there are many methods for measuring capacitance, and three common methods are listed as follows: An RC multi-resonant circuit, a capacitive sensing module of the microcontroller, and a Capacitance to Digital Converter (CDC)-based circuit.

The basic working principle of an RC multi-resonant circuit is simple. Different square wave signals change with the change of the capacitance values measured by the sensor electrodes. Then the changed square wave is compiled by the microcontroller and compared with the previous waveform to determine the change in capacitance. Because the capacitance measured by the designed sensor is approximately 1pF–3 pF (this mainly depends on the geometry and

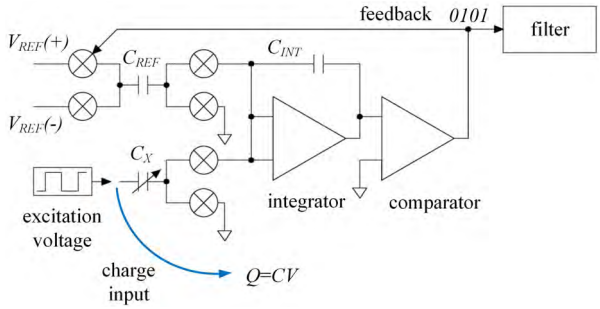

FIGURE 2. A typical schematic diagram for a Σ-Δ modulator.

size of the electrodes), the change in capacitance caused by the increasing thickness of the water film is approximately 0.1 pF–0.5 pF (this also depends on the geometry and size of the electrodes). The change in the output waveform of the RC multi-resonant circuit is relatively small, and a critical resolution of the microcontroller is required to distinguish the small capacitance changes.

A stand-alone integrated circuit typically provides higher performance than an integrated module. Analog Devices offer high-performance CDCs. These CDCs offer industry-leading measurement accuracy for measurement needs in a variety of configurations, from single capacitive sensors to capacitive sensor arrays. Considering the measurement accuracy, design cost, development time, design difficulty, and power consumption, the CDC was selected for our experiments. The basic working principle of the CDC is shown in Fig. 2. The capacitance can be converted to the voltage with a Σ-Δ modulator.

C_x refers to the measured capacitance, while C_{REF} represents an internal reference capacitor. V_{REF} represents a constant power supply. As C_x increases, the charge released by the integrator increases which leads to a greater output of the integrator. This will make the comparator to output a series of 0 and 1 that varies with the charge required by the feedback loop. Because C_{REF} is a constant capacitor, the voltage across C_{REF} increases with the increasing of C_x to balance the amount of charges. This process can be expressed as (1).

$$V = \frac{C_X \cdot V_{REF}}{C_{REF}} \tag{1}$$

In the experiment, the capacitance measurement circuit consisted of an AD7745 (CDC chip) and a PIC18F45K20 (Microcontroller). The structure diagram of the whole measurement system is shown in Fig. 3.

B. METHODOLOGY

1) SENSOR DESIGN AND OPTIMIZATION

Because it is the data acquisition unit of the measurement system, the capacitive sensor is related to the performance of the entire inspection system. The design parameters of the coplanar capacitive sensor include the electrode length (b), electrode width (a), and electrode interval (d). In this study,

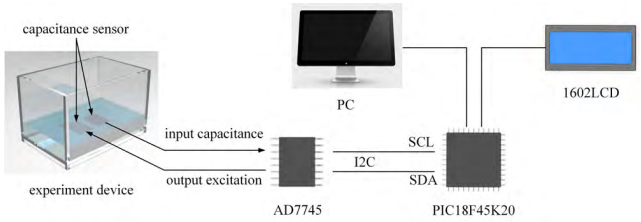

FIGURE 3. Structure diagram of the capacitance measurement system.

the penetration depth and the signal strength were selected as the indicators for the performance evaluation of the capacitive sensors.

2) PENETRATION DEPTH

The penetration depth of a capacitive sensor indicates the sensing range of the sensor. The greater the penetration depth is, the larger the sensing range is. There is no uniform definition for the penetration depth of a capacitive sensor. Therefore, it is generally evaluated by experimental measurement. In our experiment, the test block (made by HDPE) was placed in the sensing area above the capacitive sensor, and the fringing capacitance of the capacitive sensor was measured with the test block at different lift distances, as shown in Figure 4(a). Therefore, the definition of penetration depth was determined through this process. The parameters for penetration depth are: electrode length-b; electrode width-a; electrode interval-d; test block length-l; test block width-w; lift distance-h; gap between sensor and substrate-g.

The vertical distance between the test block and the surface of the capacitive sensor is the lift distance h, and the effective penetration depth of the capacitive sensor is γ.

The penetration depth $\gamma_{3\%}$ corresponds to the position h where the difference between the capacitance value C ($h = \gamma_{3\%}$) and the asymptotic capacitance value C ($h = \infty$) equals to the difference between the maximum capacitance value C ($h = 0$) and the asymptotic capacitance value C ($h = \infty$), as shown in (2) [23]:

$$C(h=\gamma_{3\%}) - C\ (h=\infty) = (C\ (h=0) - C\ (h=\infty)) \cdot 3\% \tag{2}$$

where $h = 0$ indicates that the test block is in full contact with the upper surface of the capacitive sensor, and $h = \infty$ indicates that the test block is far from the upper surface of the capacitive sensor. At this time, the change of h does not affect the capacitance between the electrodes. The trend of capacitance with different lift distances is shown in Figure 4(b).

3) SIGNAL STRENGTH

The signal strength of the sensor is the value of the fringing capacitance formed between the two traces of the capacitive sensor. It is susceptible to environmental influences because of its small fringing capacitance. A larger signal strength indicates a higher signal-to-noise ratio, which contributes to data acquisition and processing.

The capacitance variation of the coplanar capacitive sensor exhibits a nonlinear characteristic. For different coplanar

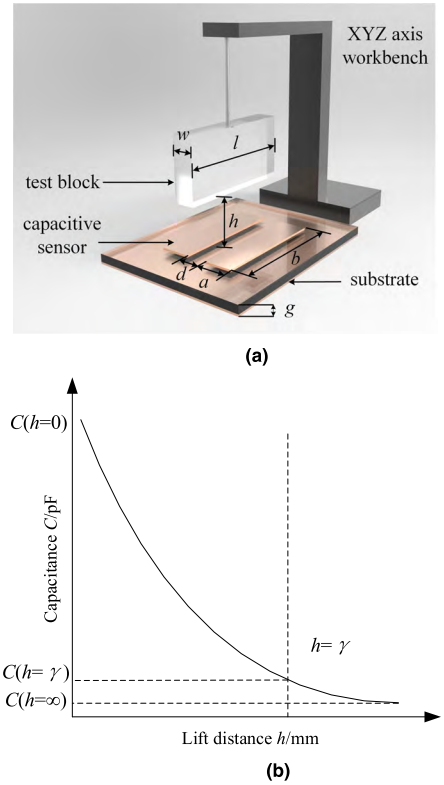

FIGURE 4. Experimental setups for the penetration depth and the changes of capacitance with different lift distances for the (a) experimental device design and (b) capacitance changing with different lift distances.

capacitive sensor structures, there is no simple unified mathematical model and formula equation. The calculation of the capacitance is only an approximate evaluation. Previous work derived a semi-analytical equation for a capacitive proximity sensor that could be used to guide the design of the parallel coplanar capacitive sensor. The capacitance can be calculated by the following equation [24]:

$$C = \eta \cdot \varepsilon \cdot b \cdot \left(\frac{a}{d}\right)^{\frac{2}{\pi}\pi \operatorname{ctan}\left(\frac{d}{b}\right)} \cdot X^{\beta} \cdot Y^{\gamma} \tag{3}$$

where X and Y are scale-independent, and η, β and γ can be calculated according to the series of experimental results. For the coplanar capacitive sensor, Equation (4) can be used for the capacitance calculation based on our previous experiments.

$$C = \frac{7}{40} \cdot \varepsilon \cdot b \cdot \left(\frac{a}{d}\right)^{\frac{1}{3}+\frac{2}{\pi}\arctan\left(\frac{d}{b}\right)} \cdot \left(1+\frac{b}{a}\right)^{\frac{1}{3}} \cdot \left(\frac{d}{a}\right)^{-\frac{1}{3}} \tag{4}$$

4) EXPERIMENTAL PLATFORM DESIGN

To verify the feasibility and the performance of the designed coplanar capacitive sensor for the detection of the water film on an insulation surface, a proper experimental platform was necessary. A sealed glass tank was set as sensing container. An ultrasound humidifier with a specific power was applied in order to generate water fog (water particles $< 10\ \mu$m). The water fog was transmitted to the tank through

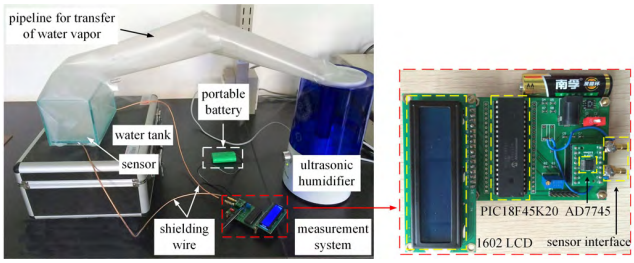

FIGURE 5. The layouts of the experimental platform and the measurement system.

a flexible pipe. With a controlled time and fixed humidifier working power, the amount of water could be estimated simply. A dual-plate coplanar capacitive sensing electrode was placed outside of the bottom surface of the tank. The layout of the experimental platform is shown in Figure 5.

Some important notes for the experiment are as follows. i) The output power and the particle size needed to be considered to ensure that the thickness of water film was controllable. ii) Anti-fogging coating needed to be applied on the inside surfaces of the glass tank, except for the bottom surface, and a long enough cooling time was necessary to ensure that all water particles could condense at the bottom surface of the tank.

The parameters of the ultrasound humidifier are listed: the power is 30W; the maximum humidification capacity is 300 ml/h; the particle size is $< 10\ \mu$m.

III. SIMULATIONS AND EXPERIMENTS

A. DETECTION OF THE SENSOR PENETRATION DEPTH

Through the simulation by COMSOL and experimental verification, the influences of the capacitive sensor parameters (electrode length b, electrode width a, and electrode interval d) and the test block length on the sensor penetration depth were studied. The gap between the sensor and the shielding substrate (g) is 5mm in both simulation and experiments. Three sets of experiments for the different electrode intervals, different test block lengths, and different electrode width-length ratios were considered.

The simulation model used in COMSOL is 3D and the parameters of model in simulation are the same as the experiment device. The relative primitivities of the material used in simulation and experiment are: $\varepsilon_{\text{air}} = 1$, $\varepsilon_{\text{glass}} = 4.2$.

The setups of the experiments are listed in Table 1, and the test system is shown in Figure 6. The capacitance was measured by an impedance analyzer (Agilent 4294A), and the excitation voltage and the frequency were set to 5 V and 32 kHz, respectively. The lifting distances range changed from 0 mm to 15 mm with by 1 mm increasing intervals. Each set of experiments was measured five times to reduce the impact of random errors and systematic errors on the measured results. The capacitive sensor and the impedance analyzer were connected by shielded wires, so the capacitance between the cables can be ignored. The SMB and BNC interfaces were used at both ends to eliminate external interference and facilitate experimental installation. The XYZ axis

TABLE 1. Setups of the experiments for the sensor penetration depth test.

Group	Electrode width a (mm)	Electrode length b (mm)	Gaps between electrodes d (mm)	Test block width w (mm)	Test block length l (mm)	Lift distance h (mm)
Experiments for different electrode intervals						
1	10	150	6	10	150	0:1:15
2	10	150	10	10	150	0:1:15
3	10	150	14	10	150	0:1:15
Experiments for different test block lengths						
1	10	150	6	10	30	0:1:15
2	10	150	6	10	90	0:1:15
3	10	150	6	10	150	0:1:15
Experiments for different electrode width-length ratios						
1	5	300	6	10	90	0:1:15
2	10	150	6	10	90	0:1:15
3	15	100	6	10	90	0:1:15

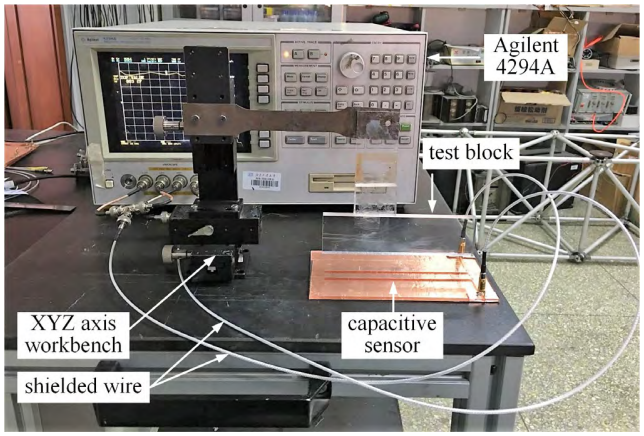

FIGURE 6. Experimental setup for the penetration depth.

workbench was used to adjust the lift distance. The normalizations for the simulation and the measurement were performed with (5), as demonstrated in Figure 7 (a), (b), and (c). The penetration depth was calculated with Equation (2), as illustrated in Figure 7 (d).

$$C_{\text{normal}} = \frac{C - C_{\min}}{C_{\max} - C_{\min}} \tag{5}$$

where C_{normal} is the normalized value and C refers to the measured or simulated capacitance. C_{max} and C_{min} are maximum and minimum values of the measured or simulated capacitances, respectively.

It is easy to conclude from Figure 7 (a) and Figure 7 (d) that when the width-to-length ratio was set to 1:15 and the length of the test block was 150 mm:

i) The capacitance between the electrodes decreased with the increase of the lifting distance h. When d was equal to 6 mm, which was smaller than the test block width (10 mm), the capacitance decreased rapidly. The trends of the simulated value were consistent with the trends of the measured value. The penetration depth was around 7 mm according to Equation (2).

ii) When d was equal to 10 mm, which was equal to the test block width, the capacitance decreased more slowly. Due to the larger gap between the sensor electrodes,

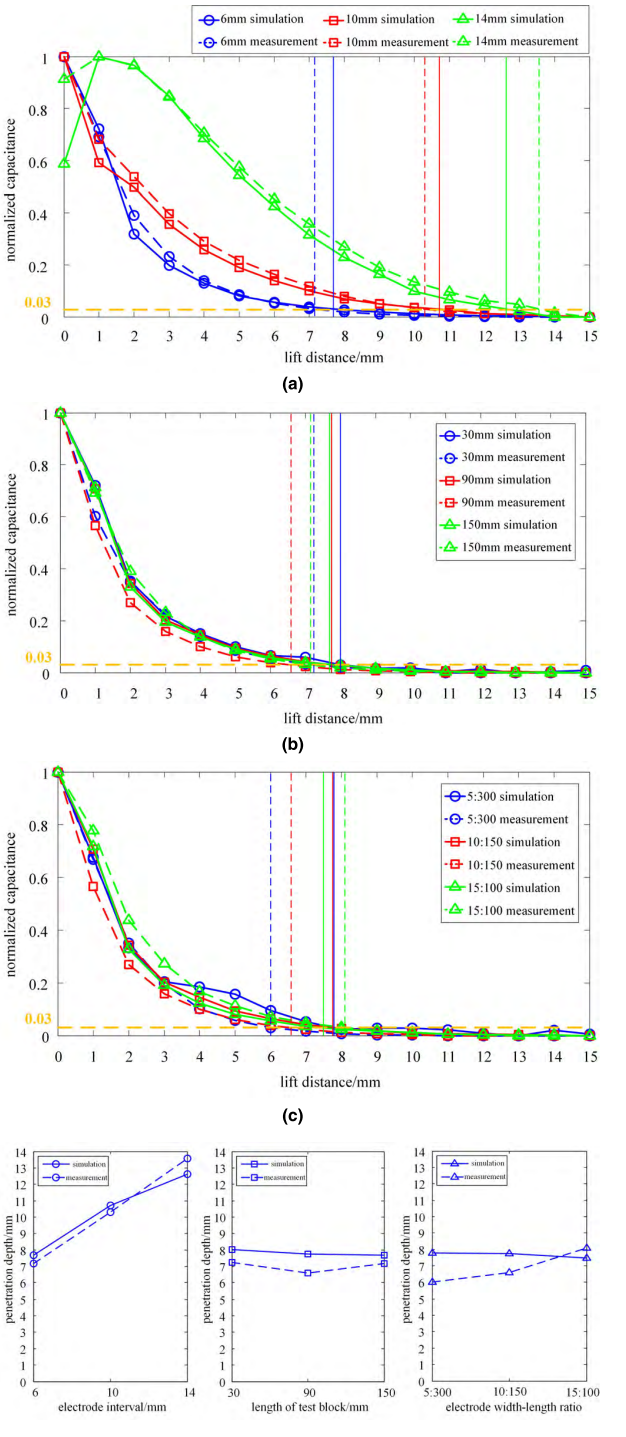

FIGURE 7. Simulated and experimental results of the measurement of the sensor penetration depth. (a) Normalized capacitance for different electrode intervals. (b) Normalized capacitance for different test block lengths. (c) Normalized capacitance for different electrode width-length ratios. (d) Changes of the penetration depth for three groups of experiments.

the sensing range of the sensor was enlarged, which also represented a deeper penetration depth. The penetration depth was approximate to 11 mm.

iii) As the electrode interval increased, $d = 14$ mm, which was larger than the test block width w, and the capacitance

first increased and then decreased. The maximum value appeared when the lifting distance $h = 1$ mm. The capacitance value was the largest, and the same trend occurred in both the simulated and measured values. However, at $h = 0$ mm, the simulated value was significantly smaller than the measured value. This was because the fabricated sensor interval was slightly less than 14 mm, resulting in a greater capacitance value than the simulated value at $h = 0$ mm. The penetration depth was approximately 13 mm.

In summary, the penetration depth of the sensor increased with the increase of the gap between the electrodes d; i.e., the electrode interval was positively correlated with the penetration depth. However, it should be noted that the sensitivity of the sensor decreased with the increase of d; i.e., the electrode interval was negatively correlated with the penetration depth.

For the second group of experiments, the width-to-length ratio was set to 1:15, and the gaps between the sensor electrodes, d, were set to 6 mm. From Figure 7 (b) and Figure 7 (d), it can be determined that:

i) For different test block lengths l, the capacitance decreased with the increase of the lift distance h, and the downward trends of the different test block lengths were consistent.

ii) As the length of the test block increased, the penetration depth of the sensor changed by a small amount, indicating that the penetration depth of the capacitive sensor was not affected by the length of the test block, and the measured value was essentially consistent with the trend of the simulated value.

From Figure 7 (c) and Figure 7 (d), it can be determined that:

i) In the case of the same electrode area and the same electrode interval, for capacitors with different width-length ratios, the capacitance decreased with the increase of the lift distance.

ii) As the electrode width-length ratio changed, the penetration depth of the measured value increased slowly, and the penetration depth of the simulated value remained essentially the same. This indicates that the width-length ratio of the capacitive sensor had little effect on the penetration depth, so it could be ignored.

For the thickness measurement of the water film on an insulation surface, the penetration depth should be larger than the thickness of the insulation surface. However, this does not mean that a greater penetration depth produces a better performance. Considering the requirement of sensor sensitivity and the suppression of the environmental influences, the penetration depth should be decided properly.

B. SIGNAL STRENGTH

We used the global optimization toolbox of Maple to calculate the design parameters of the sensor based on Equation (3). The ranges of a, b, and d were set to 6 mm - 14 mm, 60 mm – 180 mm, and 6 mm - 14 mm, respectively. Figure 8 shows the influence of the parameter combinations ab, ad, and bd on the measured capacitance of the sensor.

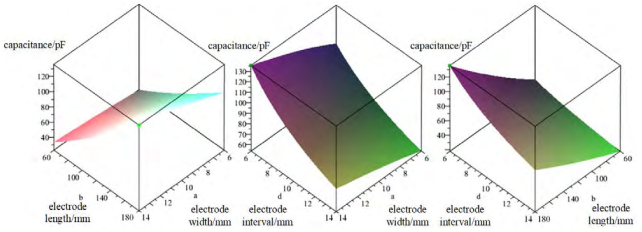

FIGURE 8. Maple Optimization results.

Some conclusions can be derived from Figure 8. The maximum value was 135.516 pF when $a = 14$ mm, $b = 180$ mm, and $d = 6$ mm. Within the above ranges of a, b, and d, the effective weights of these three parameters for the signal strength were $d > b > a$; i.e., the gap d had the greatest influence on the signal strength of the capacitive sensor, and it was negatively correlated with the signal strength. The smaller the electrode interval was, the larger the edge capacitance value was, and the stronger the signal strength was. However, from Section 3.1, it can be determined that a smaller electrode interval resulted in a smaller penetration depth. To satisfy the penetration depth and signal strength at the same time, the geometry parameter of the coplanar capacitive sensor was set to $a = 10$ mm, $b = 150$ mm, and $d = 10$ mm. The penetration depth could be measured from the experiment based on (2). This depth was 10.30 mm, and this was appropriate for the following experiments.

C. THICKNESS MEASUREMENT OF THE WATER FILM

The AD7745 based system was used to measure the capacitance changes. The testing results were compared with the simulation results of COMSOL and the measured value of Agilent 4294A. The simulation model used in COMSOL is 3D and the parameters of model in simulation are the same as the experiment device. The relative primitivities of the material used in simulation and experiment are: $\varepsilon_{\text{air}} = 1$, $\varepsilon_{\text{glass}} = 4.2$, $\varepsilon_{\text{water}} = 80$.

The experimental setups are listed as follows. For the thickness measurement of the water film, distilled water was added to the ultrasound humidifier. The tank bottom glass was 150 mm long, 100 mm wide, and 5 mm thick. The anti-frog agent was applied to the 4 inner surfaces around the glass box, so the water can only condense on the inner surface of the bottom. The anti-frog agent can last for 48h, and we used anti-frog agent before every experiment. During the experiment, the chamber is sealed. The temperature of experimental environment is room temperature (around 20°C.).

The coplanar capacitive sensor was made of flexible copper and placed under the tank on the outer surface of the bottom glass. A 5V AC source with 32kHz frequency is applied to the sensor. In a similar manner to the previous experiment for penetration depth measurement, shielded wires were used to connect the capacitive sensor and the measurement system. SMB and BNC interfaces were used at both ends to eliminate external interference and to create an installation.

TABLE 2. Comparison of the measured values from the AD7745, the impedance analyzer, and the simulated values from COMSOL.

No.	Liquid thickness (mm)	Humidifying time (s)	AD7745 measurement (fF)	Impedance analyzer measurement (fF)	Simulation (fF)
1	0	0	546.6	527.4	510.0
2	0.1	18	610.6	544.8	630.0
3	0.2	36	655.4	579.4	711.0
4	0.3	54	700.2	614.6	799.0
5	0.4	72	751.4	662.0	866.0
6	0.5	90	796.2	700.6	933.0
7	0.6	108	834.6	753.0	993.0
8	0.7	126	869.8	792.8	1045.0
9	0.8	144	902.0	838.2	1109.0
10	0.9	162	937.0	890.0	1138.0
11	1.0	180	965.8	932.8	1181.0
12	1.1	198	997.8	986.2	1229.0
13	1.2	216	1023.4	1033.0	1258.0
14	1.3	234	1058.6	1071.2	1297.0
15	1.4	252	1084.2	1105.0	1339.0
16	1.5	270	1109.8	1143.4	1372.0

Note: (water film increased from 0 mm to 1.5 mm with a 0.1 mm interval)

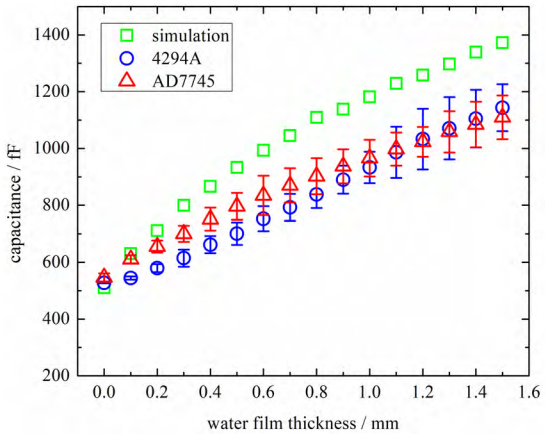

FIGURE 9. Measured capacitance changing trends.

The thickness of the water film on the bottom surface increased from 0 mm to 1.5 mm with a 0.1 mm interval. The capacitance between the electrodes were measured for 10 turns. In each turn, the capacitance from 0 mm to 1.5 mm were measured by AD7745 and impedance analyzer. The average value could reduce the influences of the random errors and the systematic errors on the measurement results. According to the output power of the humidifier, for every 0.1 mm increase of the water film on the bottom glass surface, 18 seconds of operation time as required. For each thickness, four minutes of rest time was necessary after humidification to ensure that the water particles completely deposited on the surface. The results derived from the AD7745-based system, the impedance analyzer, and the COMSOL simulation are listed in Table 2, and the comparison results are shown in Figure 9.

Some conclusions can be derived from Figure 9. i) The capacitance increased with the increasing thickness of the water film. There was a small difference between the measurements and the simulations when the thickness of the water film increased from 0 mm to 0.2 mm, and the average errors were small for all three methods. ii) When the liquid thickness was in the range of 0.3 mm to 1.3 mm, the average error range of the measured capacitance increased significantly. This was caused by the error accumulation of the water film thickness. Each increase of 0.1 mm brought more errors, and eventually the error range gradually increased. The difference between the experimental results and simulation results became larger.

IV. CONCLUSION

In this study, a coplanar capacitive sensor for water film thickness detection was designed. The thickness of the water film was measured by the self-made AD7745 detection system. The experimental measurement conditions were not exactly the same as those of the COMSOL. For a multiphysics finite element simulation, for example, the excitation frequency and ambient noise cannot be set in the COMSOL. However, these factors were presented in the actual measurement and they affected the final measurement result, so the overall difference between the measured and simulated values was acceptable. Thus, the detection system can replace an impedance analyzer in detecting the thickness of the water film, and its accuracy and reliability meet the needs of engineering applications.

The sensors were designed to define the penetration depth and the signal strength. The experiments showed that the designed sensor (size) enabled accurate measurement of the thickness of the water film.

With the detection system based on AD7745, the thickness of water film from 0mm to 1.5mm was measured and the resolution was less than 0.1mm. The accuracy and the reliability of the test were satisfactory for practical engineering applications.

REFERENCES

[1] S. T. V. Sim, S. R. Suwarno, T. H. Chong, W. B. Krantz, and A. G. Fane, "Monitoring membrane biofouling via ultrasonic time-domain reflectometry enhanced by silica dosing," *J. Membrane Sci.*, vol. 428, pp. 24–37, Feb. 2013.

[2] E. E. Franco, J. C. Adamowski, and F. Buiochi, "Ultrasonic sensor for the presence of oily contaminants in water," *Dyna*, vol. 79, no. 176, pp. 4–9, Dec. 2012.

[3] C. Zhang, Y. Huang, Y. Fang, P. Liao, Y. Wu, H. Chen, Z. Chen, Y. Deng, S. Li, H. Liu, and N. He, "The liquid level detection system based on pressure sensor," *J. Nanosci. Nanotechno.*, vol. 19, no. 4, pp. 2049–2053, Apr. 2019.

[4] A. Horsley and D. S. Thaler, "Microwave detection and quantification of water hidden in and on building materials: Implications for healthy buildings and microbiome studies," *BMC Infectious Diseases*, vol. 19, p. 67, Jan. 2019.

[5] B. Noltingk, "A novel proximity gauge," *J. Phys. E, Sci. Instrum.*, vol. 2, no. 4, p. 356, 1969.

[6] R. Tang and Y. Huang, "Cable insulation detection based on coplanar capacitive sensor," in *Proc. IEEE 32nd Youth Acad. Annu. Conf. Chin. Assoc. Automat. (YAC)*, Hefei, China, May 2017, pp. 286–291.

[7] S. G. Wang, W. Q. Wang, and H. Y. Tang, "Capacitance-type sensor system for characterizations of icing behavior," *J. Test. Eval.*, vol. 42, no. 5, pp. 1308–1314, Sep. 2014.

[8] K. Sundara-Rajan, L. Byrd, II, and A. V. Mamishev, "Moisture content estimation in paper pulp using fringing field impedance spectroscopy," *IEEE Sensors J.*, vol. 4, no. 3, pp. 378–383, Jun. 2004.

[9] A. A. Nassr, W. H. Ahmed, and W. W. El-Dakhakhni, "Coplanar capacitance sensors for detecting water intrusion in composite structures," *Meas. Sci. Technol.*, vol. 19, no. 7, Jun. 2008, Art. no. 075702.
[10] I. Matiss, "Multi-element capacitive sensor for non-destructive measurement of the dielectric permittivity and thickness of dielectric plates and shells," *NDT E Int.*, vol. 66, pp. 99–105, Sep. 2014.
[11] S. Schmidt, M. Schüßler, C. Damm, C. Schuster, and R. Jakoby, "Concept and design of a 40 GHz differential sensor for the analysis of biomedical substances," in *Proc. IEEE Topical Conf. Biomed. Wireless Technol., Netw., Sens. Syst. (BioWireleSS)*, Austin, TX, USA, Jan. 2016, pp. 52–54.
[12] B. Axt, S. Zhang, and R. Rajamani, "Wearable coplanar capacitive sensor for measurement of water content—A preliminary endeavor," *J. Med. Devices*, vol. 10, no. 2, Jun. 2016, Art. no. 020953.
[13] M. Carminati, L. Pedalá, E. Bianchi, F. Nason, G. Dubini, L. Cortelezzi, G. Ferrari, and M. Sampietro, "Capacitive detection of micrometric airborne particulate matter for solid-state personal air quality monitors," *Sens. Actuators A, Phys.*, vol. 219, pp. 80–87, Nov. 2014.
[14] M. Carminati, P. Ciccarella, M. Sampietro, and G. Ferrari, "Single–chip CMOS capacitive sensor for ubiquitous dust detection and granulometry with sub-micrometric resolution," in *Convegno Nazionale Sensori*. Cham, Switzerland: Springer, 2016, pp. 8–18.
[15] Q. Yang, J. Y. Andrew, J. Simonton, G. Yang, Y. Dohrmann, Z. Kang, Y. Li, J. Mo, and F. Y. Zhang, "An inkjet-printed capacitive sensor for water level or quality monitoring: Investigated theoretically and experimentally," *J. Mater. Chem. A*, vol. 5, no. 34, pp. 17841–17847, Sep. 2017.
[16] L. W. Lim, F. Aziz, Z. Ahmad, N. A. Roslan, A. Supangat, and K. Sulaiman, "Planar capacitive type humidity sensor fabricated using PTB7-Th by facile solution processing approach," *Appl. Phys. A*, vol. 125, no. 1, p. 16, Jan. 2019.
[17] K. Chetpattananondh, T. Tapoanoi, P. Phukpattaranont, and N. Jindapetch, "A self-calibration water level measurement using an interdigital capacitive sensor," *Sens. Actuators A, Phys.*, vol. 209, pp. 175–182, Mar. 2014.
[18] A. Rivadeneyra, J. Fernández-Salmerón, J. Banqueri, J. A. López-Villanueva, L. F. Capitan-Vallvey, and A. J. Palma, "A novel electrode structure compared with interdigitated electrodes as capacitive sensor," *Sens. Actuators B, Chem.*, vol. 204, pp. 552–560, Dec. 2014.
[19] Z. Li, G. Chen, Y. Gu, K. Wang, W. Li, and X. Yin, "Further investigations into the capacitive imaging technique using a multi-electrode sensor," *Appl. Sci.*, vol. 8, no. 11, p. 2296, Nov. 2018.
[20] R. T. Sheldon and N. Bowler, "An interdigital capacitive sensor for non-destructive evaluation of wire insulation," *IEEE Sensors J.*, vol. 14, no. 4, pp. 961–970, Apr. 2014.
[21] X. Yin, D. A. Hutchins, G. Chen, and W. Li, "Investigations into the measurement sensitivity distribution of coplanar capacitive imaging probes," *NDT E Int.*, vol. 58, pp. 1–9, Sep. 2013.
[22] N. Li, M. Cao, K. Liu, C. He, and B. Wu, "A boundary detecting method for post-tensioned pre-stressed ducts based on Q-factor analysis," *Sens. Actuators A, Phys.*, vol. 248, pp. 88–93, Sep. 2016.
[23] X. B. Li, S. D. Larson, A. S. Zyuzin, and A. V. Mamishev, "Design principles for multichannel fringing electric field sensors," *IEEE Sensors J.*, vol. 6, no. 2, pp. 434–440, Apr. 2006.
[24] N. Li, H. Zhu, W. Wang, and Y. Gong, "Parallel double-plate capacitive proximity sensor modelling based on effective theory," *AIP Adv.*, vol. 4, no. 2, Feb. 2014, Art. no. 027119.

NAN LI (M'13) received the B.S. degree from Xidian University, in 2004, the M.Sc. degree from the University of Manchester, in 2008, and the Ph.D. degree from Xidian University, in 2010.

From 2010 to 2015, he was an Associate Professor with the Beijing University of Technology, Beijing, China. Since 2016, he has been an Associate Professor with Northwestern Polytechnical University, Xi'an, China. His main research interests include non-destructive testing and evaluation, sensor design and automatic control, and process tomography.

Dr. Li is a member of the International Society for Industrial Process Tomography (ISIPT) and the China Instrument and Control Society.

MINGCHEN CAO received the B.S. degree from Beijing Information Science and Technology University, in 2013, and the M.S. degree from the Beijing University of Technology, in 2016. He is currently pursuing the Ph.D. degree with Xi'an Jiaotong University. His main research interests include non-destructive testing and evaluation, and automatic control.

XIAOJUN YU received the Ph.D. degree from Nanyang Technological University, Singapore, in 2015, where he was a Postdoctoral Research Fellow, from January 2015 to August 2017. He is currently an Associate Professor with Northwestern Polytechnical University, China. His main research interests include highresolution optical coherence tomography and its imaging applications.

JIABIN JIA (M'15) was born in Inner Mongolia, China, in 1980. He received the B.Eng. and master's degrees in electrical and electronics engineering from Wuhan University, China, in 2002 and 2005, respectively, and the Ph.D. degree from the University of Leeds, in 2010, supported by the Overseas Research Students Awards Scheme Award, in 2006. He was with H3C Technology Company Ltd., as a Hardware Engineer, for one year. He was a Research Fellow with an EPSRC Project for three years. In 2013, he was appointed as a Lecturer with the School of Engineering, The University of Edinburgh. His current research interests include electrical tomography, multiphase flow measurement, instrument development, and medical imaging.

YUNJIE YANG (M'13) received the B.Eng. degree from Anhui University, China, in 2010, the M.Sc. degree from Tsinghua University, China, in 2013, and the Ph.D. degree from The University of Edinburgh, U.K., in 2018. After his Ph.D., he briefly worked as a Postdoctoral Research Associate in chemical species tomography with The University of Edinburgh, where he has become a Chancellor's Fellow in Data-Driven Innovation, since September 2018. His research interests include the areas of sensing and imaging with miscellaneous tomography modalities, and machine learning techniques for process analysis. He was a recipient of the 2015 IEEE I&M Society Graduate Fellowship Award. He has been an Associate Editor of IEEE Access, since 2019.